Irregular Solution Thermodynamics of Wood Pulp in the Superbase Ionic Liquid [*m*-TBDH][AcO]

Gordon W. Driver* and Ilkka Kilpeläinen

Electronic Supplementary Information (ESI)

Table of Contents

1. MATERIALS

m-TBDH synthesized in-house was distilled under inert conditions prior to use.[1] Acetic acid (HoneyWell, 99.8%) was used as received. [m-TBDH][AcO] was freshly prepared in ~5-10g batches prior to enocell solution preparation. Encocell paper stored under ambient conditions, was manually shredded and weighed into to an aliquot of the freshly prepared IL, followed by stirring with heating maintained at ~85°C until dissolution was complete.

2. EXPERIMENTS WITH MODULATED DIFFERENTIAL SCANNING CALORIMENTRY (MDSC) ON A TA INSTRUMENTS Q200 DSC

MDSC Description and Theory in Brief[2]

Differential scanning calorimetry (DSC), provides a thermal analysis through measurement of heat flow and temperature, where a stable, rectilinear baseline is required in order to yield high accuracy average heat flow rates, dQ/dT.

MDSC removes the dependence on baseline stability for accuracy by employing instead the measurement of the reversing heat capacity (rev-C_p), which depends only on the amplitude of the modulated heat flow, not on an average value, as is the case for traditional DSC. Here, total heat flow is obtained from the average modulated heat flow, as determined by FT analysis on the sine wave characterised by the sinusoidal modulation. Thereby, calibration of the required modulation period is necessary, as is the setting of the modulation amplitude.

A typical heating profile for MDSC is given below in Figure F1.[2]

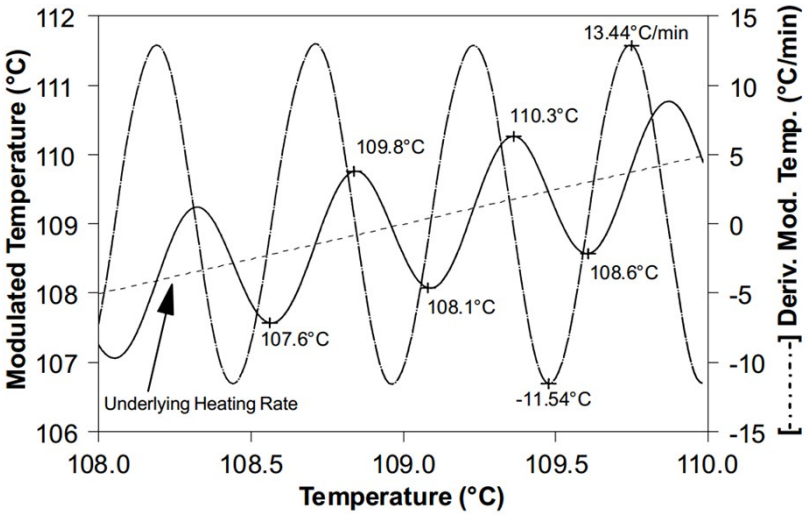

Figure F1. Sinusoidal heat profile example with using a heating rate of 1 °C/min., modulation period of 30s and a modulation amplitude of ± 1 °C.[2]

The modulated heating profile presented in Figure F1 above indicates two experiments being run in one, with both a traditional average heating rate (dashed line) and a sinusoidal heating rate (dashed – dot line) oscillating between +13.44 °C and -11.54 °C.

For experiments carried out in this work, using a pre-set modulation amplitude of ± 0.5 °C, MDSC rev-C_p calibrations were run using modulation periods of 30, 40, 60, 80 and 100 seconds. Using data presented in Table S1 below, we found the optimal modulation period to be 80 seconds.

Table S1: Reversing heat capacity calibration results

Modulation amplitude = ± 0.05 °C					
Modulation period /s	30	40	60	80	100
Rev-C_p /(J/g)/°C	1.07	1.33	1.55	1.62	1.65

For the samples investigated in this work, experiments were run in independent triplicates, with a total experiment time of 1112 min./experiment, with heating/cooling ramps of 3 °C/min. A typical run employed 4 segments: a heating mode to 100 °C to remove thermal and mechanical history, a cooling mode to -80 °C, with an isothermal mode of several hours applied, followed by a final heating mode to 100 °C.

Figure F2 below shows thermograms obtained for samples of neat [m-TBDH][AcO] and [m-TBDH][AcO] solution with encocell.

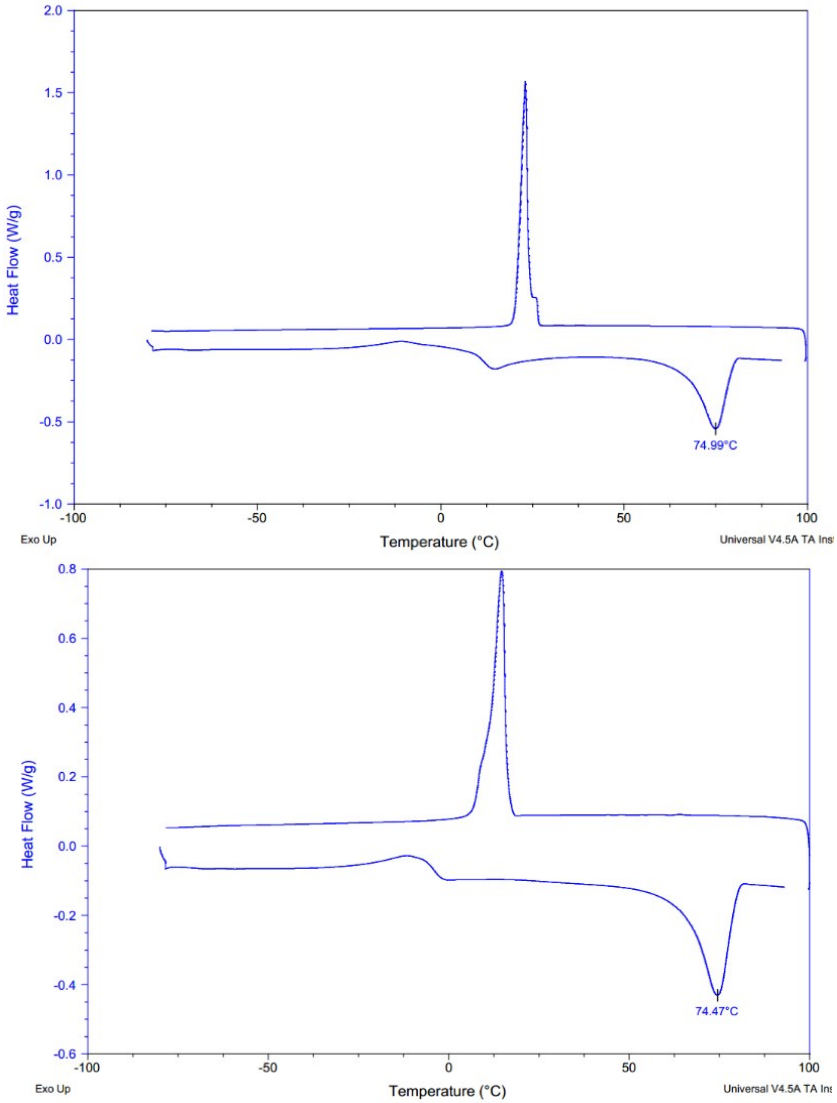

Figure F2. Thermograms of: (top) neat [m-TBDH][AcO]; (bottom) [m-TBDH][AcO] with w_i = 0.00841 encocell.

The liquid state isobaric heat capacity was taken from baseline segments preceding/exceeding the melting temperature, by up to 40 °C. The change of heat capacity for fusion, ΔC_p, was determined using $\Delta C_p = C_p$-liquid – C_p-solid, and applied to calculations using Eq 1. (see main text) as shown in Table S2 following.

Table S2: Determination of ΔC_p of solvent-*j* [m-TBDH][AcO]

Phase	*T*-range /K	[a]C_p – solid J g^{-1} deg.$^{-1}$	[b]± std. dev.	[a]C_p – liquid J g^{-1} deg.$^{-1}$	[b]± std. dev.
solid	223.15 – 263.15	1.25	0.0532		
liquid	353.15 – 365.15			2.40	0.0893
$\Delta C_p = C_p$ – liquid - C_p – solid = 1.14 J g^{-1} deg.$^{-1}$					

[a] mean of $n = 3$ measurements = $\bar{x}$, [b] ± standard deviation, $s = \sqrt{\sum_{i=1}^{n}(x_i - \bar{x})^2 \Big/ (n-1)}$

Table S3: Depression of freezing point results for solutions of enocell in [m-TBDH][AcO]

IL batch	[c]x_i	[d]w_i	[e]T /K	[f]± std. dev. /K	[g]a_j
1 [a,b]m.p. = 347.80 K ± 0.322 K	0.0111	0.00841	347.44	± 0.176	0.995
	0.0244	0.0190	344.21	± 0.0361	0.950
2: [a]m.p. = 352.12 K ± 0.01 K	0.146	0.115	333.08	± 0.0300	0.788

[a] mean of $n = 3$ measurements = $\bar{x}$, ± standard deviation, $s = \sqrt{\sum_{i=1}^{n}(x_i - \bar{x})^2 \Big/ (n-1)}$, [b] $H_{fus.}$ = 68.3 J g^{-1} ±7.13 J g^{-1} (see Eq. 1 main text), [c] mole fraction-*i* [d] mass fraction solute-*i*, [e] melting temperature of mixture, mean of 3 measurements, [f] standard deviation, $s = \sqrt{\sum_{i=1}^{n}(x_i - \bar{x})^2 \Big/ (n-1)}$, [g] solvent-*j* activities using Eq 1. (see main text).

3. THERMODYNAMIC PROCEDURE AND METHODS

Using Eq 1. (see main text) solvent-*j* activities were obtained for each composition for Table S3 above. For each mass fraction composition, the value of a_j at different temperatures was computed using Eq 2. (see main text).

3a. CALCULATIONS

Step 1. – Solvent activities a_j, at the fusion temperature

Using data reported in Tables S2 and S3 and Eq 1. (see main text) values of a_j were calculated, as given in Table S3 above.

Step 2. – Scaling of a_j from temperature *T* to some other temperature *T*' of interest

a) we require the relative partial molar enthalpy $\overline{H}_j$ of the solvent-*j,* given as $-RT^{2\partial} \big/ \partial T ln(a_{j(T)})$ (see Eq. 2 main text) where $\overline{H}_j = \overline{H}_j(T') - \overline{C_{pj}}(T - T')$, with $\overline{H}_j(T')$ the relative partial molar enthalpy at temperature T', and $\overline{C_{pj}}$ the relative partial heat capacity of solvent-*j*.

b) simple rearrangement yields $\overline{H}_j(T') = \overline{H}_j + \overline{C_{pj}}(T - T') = -RT^{2\partial} \big/ \partial T ln(a_{j(T)})$.

c) using data given in Tables S2 and S3, the pure solvent fusion temperature, $T_{fus.}$, the depressed freezing point temperature, T, and the desired temperature, T', values for $a_j(T')$ are obtained, yielding corresponding activity coefficients *via* $\Omega_j = a_j(T') \big/ w_j$

Step 3. – Processing using the Gibbs-Duhem relation[3]

Step 3a. – plots of $w_j \big/ w_i$ versus $-ln(\Omega_j)$ were prepared and fitted using cubic spline interpolation, producing good fits with coefficients of determination $R^2 > 0.997$. The curve was then integrated according

to Eq. 3 (see main text) yielding initial values of Ω_i.[3] The curve produced from such a plot is, on the solvent side, asymptotic to the *y*-axis, where w_j/w_i tends to infinity as w_i tends to zero. Such behaviour introduces mathematical complications where the area closing off the curve is unknown, as the pure solvent composition is approached, and therefore requires extrapolation, often estimated using an extrapolation function producing unsatisfactory results. An ingenious solution to this problem was beautifully presented, already in 1960, by Lakhanpal and Conway.[3] Therein, the authors exploited the fact that the unknown curve area was equivalent to an experimentally known quantity, that was merely used to incrementally increase initial values of Ω_i.

Step 3b. – the solution of Lakhanpal and Conway was employed producing the final values of Ω_i.[3] The entire procedure was then repeated, using the corrected values of Ω_i, to back-calculate values of Ω_j. It is noted that difficulties connected to the asymptotic behaviour on the solvent side are not found on the solute side. In that case, when $w_i/w_j = 0$, the integrated function becomes zero.

Step 3c. – the percentage difference between experimentally determined Ω_j and those back-calculated using Ω_i, *i.e.* $\Omega_j^{'}$, was calculated using $\left(2\left(\Omega_j - \Omega_j^{'}\right)/\Omega_j + \Omega_j^{'}\right) \cdot 100$. In this way the computed values of Ω_i are verified by the extent they provide satisfactory $\Omega_j^{'}$ values. Results obtained using these methods are given in the following section.

3b. RESULTS

Table S4: Experimentally determined molar and partial molar Gibbs energies and activity coefficients $\Omega_{i,j}$ for a binary mixture of enocell-*i* and [m-TBDH][AcO]-*j* - variation of temperature at constant mass fraction $w_i = 0.00841$

T /K	G_{mix} /kJ mol^{-1}	$G_{ideal,i}$ /kJ mol^{-1}	$G_{ideal,j}$ /kJ mol^{-1}	$G_{excess,i}$ /kJ mol^{-1}	$G_{excess,j}$ /kJ mol^{-1}	Ω_i	Ω_j
357.15	0.256	-0.119	-0.0249	0.000287	0.400	1.01	1.15
358.15	0.295	-0.120	-0.249	0.00130	0.438	1.05	1.16
359.15	0.335	-0.120	-0.250	0.00319	0.476	1.14	1.17
360.15	0.378	-0.120	-0.0251	0.00623	0.517	1.28	1.19
363.07	0.494	-0.121	-0.0252	0.0121	0.629	1.61	1.23
373.15	0.883	-0.125	-0.0260	0.0336	1.00	3.63	1.38

Table S5: Experimentally determined molar and partial molar Gibbs energies and activity coefficients $\Omega_{i,j}$ for a binary mixture of enocell-*i* and [m-TBDH][AcO]-*j* - variation of temperature at constant mass fraction $w_i = 0.0190$

T /K	G_{mix} /kJ mol^{-1}	$G_{ideal,i}$ /kJ mol^{-1}	$G_{ideal,j}$ /kJ mol^{-1}	$G_{excess,i}$ /kJ mol^{-1}	$G_{excess,j}$ /kJ mol^{-1}	Ω_i	Ω_j
357.15	0.124	-0.220	-0.0548	0.00815	0.391	1.16	1.14
358.15	0.162	-0.221	-0.0549	0.0111	0.427	1.22	1.16
359.15	0.201	-0.221	-0.0551	0.0160	0.462	1.33	1.17
360.15	0.243	-0.222	-0.0552	0.0235	0.497	1.52	1.18
363.07	0.357	-0.224	-0.0557	0.0387	0.598	1.99	1.22
373.15	0.738	-0.230	-0.0572	0.0932	0.932	5.02	1.36

Table S6: Verification of Ω_i determined by the Gibbs-Duhem relation: back-calculated Ω_j' using Ω_i values obtained for mass fraction $w_i = 0.00841$

T /K	Ω_j	Ω_i	Ω_j'	[a] % difference
357.15	1.15	1.01	1.15	-
358.15	1.16	1.05	1.16	-
359.15	1.17	1.14	1.17	-
360.15	1.19	1.28	1.19	-
363.07	1.23	1.61	1.23	-
373.15	1.38	3.63	1.37	0.727

[a] % difference = $\left(2\left(\Omega_j - \Omega_j'\right) \Big/ \Omega_j + \Omega_j'\right) \cdot 100$

Table S7: Verification of Ω_i determined by the Gibbs-Duhem relation: back-calculated Ω_j' using Ω_i values obtained for mass fraction $w_i = 0.0190$

T /K	Ω_j	Ω_i	Ω_j'	[a] % difference
357.15	1.14	1.16	1.14	-
358.15	1.16	1.22	1.16	-
359.15	1.17	1.33	1.17	-
360.15	1.18	1.52	1.18	-
363.07	1.22	1.99	1.22	-
373.15	1.36	5.02	1.36	-

[a] % difference = $\left(2\left(\Omega - \Omega_j'\right) \Big/ \Omega_j + \Omega_j'\right) \cdot 100$

Table S8: Verification of Ω_i determined by the Gibbs-Duhem relation: back-calculated Ω_j' using Ω_i values obtained for mass fraction $w_i = 0.115$

T /K	Ω_j	Ω_i	Ω_j'	[a] % difference
357.15	1.09	2.39	1.09	-
358.15	1.10	2.80	1.09	0.913
359.15	1.11	3.46	1.09	1.818
360.15	1.11	4.57	1.10	0.905
363.07	1.13	8.53	1.10	2.691
373.15	1.19	72.3	1.13	5.17

[a] % difference = $\left(2\left(\Omega_j - \Omega_j'\right) \Big/ \Omega_j + \Omega_j'\right) \cdot 100$

Table S9: Experimentally determined molar and partial molar entropies for a binary mixture of enocell-*i* and [m-TBDH][AcO]-*j* - variation of temperature at constant mass fraction $w_i = 0.00841$

T /K	$-TS_{mix}$ /kJ mol^{-1}	S_{mix} /J K^{-1} mol^{-1}	$S_{ideal,i}$ /J K^{-1} mol^{-1}	$S_{ideal,j}$ /J K^{-1} mol^{-1}	$S_{excess,i}$ / J K^{-1} mol^{-1}	$S_{excess,j}$ / J K^{-1} mol^{-1}
357.15	14.0	-39.2	0.334	0.0696	-2.125	-37.5
358.15	14.0	-39.2	0.334	0.0696	-2.122	-37.5
359.15	14.1	-39.2	0.334	0.0696	-2.122	-37.5
360.15	14.1	-39.2	0.334	0.0696	-2.124	-37.5
363.07	14.2	-39.2	0.334	0.0696	-2.123	-37.5
373.15	14.6	-39.2	0.334	0.0696	-2.123	-37.5

Table S10: Experimentally determined molar and partial molar entropies for a binary mixture of enocell-*i* and [m-TBDH][AcO]-*j* - variation of temperature at constant mass fraction $w_i = 0.0190$

T /K	$-TS_{mix}$ /kJ mol^{-1}	S_{mix} /J K^{-1} mol^{-1}	$S_{ideal,i}$ /J K^{-1} mol^{-1}	$S_{ideal,j}$ /J K^{-1} mol^{-1}	$S_{excess,i}$ / J K^{-1} mol^{-1}	$S_{excess,j}$ / J K^{-1} mol^{-1}
357.15	13.7	-38.4	0.153	0.617	-5.41	-33.7
358.15	13.8	-38.4	0.153	0.617	-5.40	-33.8
359.15	13.8	-38.4	0.153	0.617	-5.40	-33.8
360.15	13.8	-38.4	0.153	0.617	-5.41	-33.8
363.07	13.9	-38.4	0.153	0.617	-5.40	-33.8
373.15	14.3	-38.4	0.153	0.617	-5.40	-33.8

Table S11: Experimentally determined molar and partial molar entropies for a binary mixture of enocell-*i* and [m-TBDH][AcO]-*j* - variation of temperature at constant mass fraction $w_i = 0.115$

T /K	$-TS_{mix}$ /kJ mol^{-1}	S_{mix} /J K^{-1} mol^{-1}	$S_{ideal,i}$ /J K^{-1} mol^{-1}	$S_{ideal,j}$ /J K^{-1} mol^{-1}	$S_{excess,i}$ / J K^{-1} mol^{-1}	$S_{excess,j}$ / J K^{-1} mol^{-1}
357.15	32.1	-89.8	2.07	0.896	-77.5	-15.2
358.15	32.1	-89.7	2.07	0.896	-77.5	-15.2
359.15	32.2	-89.7	2.07	0.896	-77.4	-15.2
360.15	32.3	-89.8	2.07	0.896	-77.5	-15.2
363.07	32.6	-89.8	2.07	0.896	-77.5	-15.2
373.15	33.5	-89.7	2.07	0.896	-77.5	-15.2

REFERENCES

1. Helminen, J.; King, A. Kilpeläinen, I.; World Patent, WO 2019/092319 Al, 2018.

2. http://www.tainstruments.com/pdf/literature/MDSC.pdf

3. M. L. Lakhanpal and B. E. Conway, *Can. J. Chem.*, 1960, 38, 199–203.